

Phase structure and thermal behaviour of polypropylene/hydrogenated polycyclopentadiene blends

Ezio Martuscelli

Istituto di Ricerche su Tecnologia dei Polimeri e Reologia del CNR, Via Toiano 6, 80072 Arco Felice, Naples, Italy

and Maurizio Canetti and Alberto Seves

Stazione Sperimentale per la Cellulosa, Piazza Leonardo da Vinci 26, 20133 Milan, Italy
(Received 18 January 1988; revised 24 June 1988; accepted 3 August 1988)

Isothermally crystallized blends of isotactic polypropylene (iPP) with saturated polycyclopentadiene (PCP) were examined by differential scanning calorimetry and wide- and small-angle X-ray scattering. The presence of PCP did not interfere with the apparent crystal size, and a possible correction by paracrystallinity or microstrain did not produce a significant difference. The long period increased as a function of PCP content, which suggests its distribution in the interlamellar regions. The samples were subjected to chloroform extraction. This solvent, able to remove the PCP fraction, produces a rearrangement of the remaining iPP structure. The crystallinity and apparent crystal size did not change, whereas the microstrain correction became more significant. The long period assumed a new value which was the same for all extracted blends. Density measurements showed swelling of the amorphous phase. The specific volumes of the extracted blends depended on the initial PCP content.

(Keywords: polypropylene; polycyclopentadiene; blends; phase structure; density; small-angle X-ray scattering; wide-angle X-ray scattering; solvent extraction)

INTRODUCTION

The thermal and crystallization behaviour of blends of isotactic polypropylene (iPP) and saturated polycyclopentadiene (PCP) was investigated in a previous work¹. Examination by optical microscopy of isothermally crystallized films showed that the blends were completely filled with spherulites, and no segregation phenomenon of PCP was observed. The dilution of iPP with PCP caused a depression of the spherulite growth rate and of the overall kinetic rate constant. These depressions were greater with increasing concentration of the non-crystallizable component and for decreasing undercooling. The glass transition temperature of the blends increased with PCP concentration, in good agreement with the Fox equation. For a large range of undercooling values, the melting temperature increases linearly with the crystallization temperature for plain iPP and blends. In addition, the equilibrium melting temperature decreases with PCP concentration. The Flory-Huggins interaction parameter is negative and close to zero. These observations led the authors to conclude that iPP and PCP are compatible in the melt. The object of the present work was to obtain some structural information about PCP dispersion in the blend and about its possible interference with iPP crystallization, in terms of iPP crystal dimensions. Furthermore, interaction with the blends of a solvent, able to remove the non-crystallizable component, was also analysed. Extraction of a predetermined PCP fraction can be used to obtain a polypropylene with new structure and morphology. Both small- and wide-angle X-ray scattering (SAXS, WAXS)

techniques have already been used in previous work to evaluate long period crystal size values and other structural parameters of polymers and blends isothermally crystallized^{2,3}.

EXPERIMENTAL

Materials

Binary blends of isotactic polypropylene (Moplen T30S, M_w 300 000; Montedison) and saturated polycyclopentadiene (Escorez, M_w 630; Esso Chemical) were prepared by mixing the polymers in a microextruder. The weight mixing ratios of polypropylene/polycyclopentadiene (iPP/PCP) were: 90/10, 70/30 and 50/50. Blends and pure iPP were melted at 200°C for 10 min, then isothermally crystallized at 123°C. All samples were extracted with chloroform in Soxhlet to constant weight. Seven hours were enough to remove over 95% of the PCP fraction. Before and after extraction, the samples were analysed by differential scanning calorimetry (d.s.c.), WAXS and SAXS techniques.

Differential scanning calorimetry (d.s.c.)

The samples were analysed by a Perkin-Elmer DSC-4/Thermal Analysis Data Station (TADS) system. The samples (about 4 mg) were heated from 30 to 200°C at a scanning rate of 10°C min⁻¹. The apparent enthalpies of fusion and the melting temperatures were obtained from the area and the maximum of the endothermic peaks.

Density measurements

The density of PCP was measured by flotation at 25°C in an aqueous potassium iodide solution⁴. The density of the extracted samples was evaluated with a capillary dilatometer filled with mercury at 25°C⁵.

Wide-angle X-ray scattering

The WAXS line-broadening data were obtained by a Siemens D-500 diffractometer, with a Siemens FK 60-10, 2000 W Cu tube and with a scanning rate of 10 min per degree (2θ). The samples were mounted on a specimen carrier for specimen spinning with a rotational speed of 30 rpm. A nickel standard sample was employed to determine the instrumental broadening.

Small-angle X-ray scattering

The SAXS measurements were obtained by a Huber 701 small-angle chamber that consists of two glass blocks; the distance between them was 15 μm . One of the glass blocks functions as a monochromator by total reflection⁶. The radiation was Cu K_α ($\lambda = 1.542 \text{ \AA}$). The diffracted intensity was measured using a scintillation counter with a Scintiflex 25 YB photomultiplier with a beryllium window and NaI(Tl) crystal. The scans were started at $2\theta = 0.08^\circ$ with steps of $2\theta = 0.015^\circ$. The selected time of 600 s was sufficient to obtain a good number of counts in the low scattering region. The raw data were first corrected for sample absorption, and then the background was subtracted. After smoothing, the collimation error was removed by applying the Glatter method⁷ to obtain desmeared scattering data.

RESULTS AND DISCUSSION

Thermal behaviour

The apparent enthalpies of fusion ΔH^* of plain iPP and blends were calculated from the area of the d.s.c. endothermic peaks. The crystalline and amorphous weight fractions were calculated from the following relations:

$$w_{\text{cr}} = \Delta H^* / \Delta H_{\text{PP}} \quad w_{\text{am}} = (1 - w_{\text{cr}})$$

where ΔH_{PP} (44 cal g^{-1}) is the heat of melting per gram of 100% crystalline iPP⁸.

The weight fraction crystallinity decreased as a function of PCP content, whereas, as expected, after extraction an almost constant value (similar to that of pure iPP) was found for all samples (Table 1). The crystalline and amorphous volume fractions (ϕ_{cr} and ϕ_{am}) can be determined from these data and from density

Table 1 Amorphous and crystalline fractions of plain iPP and blends before and after extraction: by weight (w) and by volume (ϕ)

iPP/PCP	w_{am}	w_{cr}	ϕ_{am}	ϕ_{cr}
Before extraction				
100/0	0.47	0.53	0.50	0.50
90/10	0.56	0.44	0.58	0.42
70/30	0.62	0.38	0.62	0.38
50/50	0.71	0.29	0.70	0.30
Extracted				
100/0	0.45	0.55	0.52	0.48
90/10	0.49	0.51	0.60	0.40
70/30	0.51	0.49	0.67	0.33
50/50	0.47	0.53	0.74	0.26

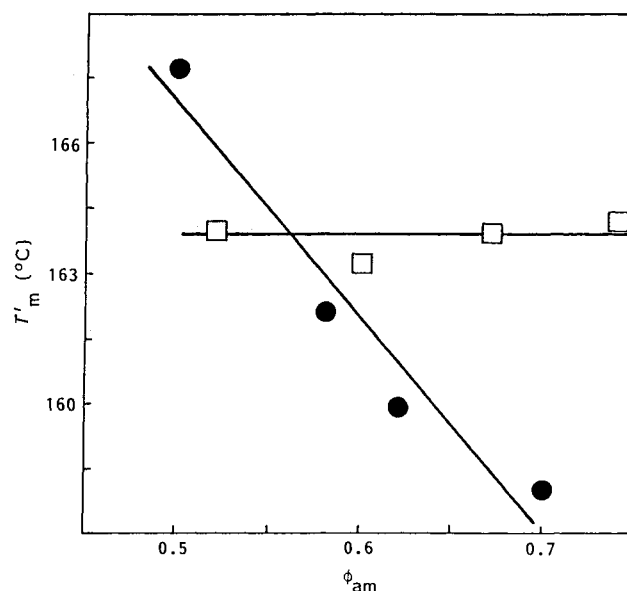


Figure 1 Melting points versus amorphous volume fraction before (●) and after (□) chloroform extraction

measurements. As shown by the data reported in Table 1, ϕ_{cr} and ϕ_{am} of corresponding samples before and after extraction have practically the same values. This indicates that after extraction of PCP the overall volume of blend samples is left almost unchanged.

Plots of the observed calorimetric melting temperature (T'_m) against ϕ_{am} for plain iPP and iPP/PCP blends before and after extraction are shown in Figure 1. It can be observed that T'_m , for non-extracted blend samples, decreases linearly with ϕ_{am} . Such a trend is in agreement with the crystallization behaviour reported in ref. 1 where compatibility in the melt at molecular level of iPP and PCP was suggested.

Extracted blends show values of T'_m that are independent of ϕ_{am} and are practically equal to that of plain iPP exposed to the solvent action of chloroform. Moreover, these T'_m values are all lower and higher than those of non-extracted plain iPP and blends respectively (see Figure 1). The trends of the plots of Figure 1 can be explained only by taking into account the WAXS and SAXS results reported in the next sections of this paper.

Density measurements

The crystalline and amorphous volume fractions of the non-extracted blends were calculated from:

$$\phi_{\text{cr}} = \frac{(w_{\text{cr}} V_{\text{s,cr}})}{V_{\text{s,blend}}} \quad \phi_{\text{am}} = \frac{(w_{\text{am,PP}} V_{\text{s,am,PP}}) + (w_{\text{PCP}} V_{\text{s,PCP}})}{V_{\text{s,blend}}}$$

where the PCP specific volume $V_{\text{s,PCP}}$ measured by flotation⁴ is 0.926 $\text{cm}^3 \text{g}^{-1}$; the amorphous and crystalline iPP specific volumes⁸ $V_{\text{s,am,PP}}$, $V_{\text{s,cr}}$ are respectively 1.177 and 1.053 $\text{cm}^3 \text{g}^{-1}$; w_{cr} is the crystalline weight fraction of iPP calculated by d.s.c.; w_{PCP} is the known weight fraction of PCP; and the amorphous iPP weight fraction can be easily obtained from:

$$w_{\text{am,PP}} = 1 - (w_{\text{cr}} + w_{\text{PCP}})$$

The specific volume values were calculated for the blends from:

$$V_{\text{s,blend}} = (w_{\text{cr}} V_{\text{s,cr}}) + (w_{\text{am,PP}} V_{\text{s,am,PP}}) + (w_{\text{PCP}} V_{\text{s,PCP}})$$

For pure iPP the same relations were applied; the PCP contribution was obviously ignored. The PCP fraction was almost completely removed by chloroform extraction. Assuming an unchanged crystal density, the amorphous volume fraction of the extracted samples was calculated according to the relation:

$$\phi_{am} = 1 - \left(\frac{w_{cr} V_{s,cr}}{V_{s,x}} \right)$$

where $V_{s,x}$ is the total sample specific volume calculated by capillary densimetry⁵. The mercury, employed as filler medium, was unable to diffuse into the swollen amorphous phase.

The extraction did not substantially modify the volume fractions of amorphous and crystalline phases (Table 1).

For non-extracted samples, the amorphous phase densities were calculated from:

$$d_{am} = 1/(\gamma_{PCP} V_{s,PCP}) + (\gamma_{am,PP} V_{s,am,PP})$$

where γ_{PCP} and $\gamma_{am,PP}$ are the polymer weight fractions in the amorphous phase, calculated by:

$$\gamma_{PCP} = \frac{w_{PCP}}{w_{PCP} + w_{am,PP}} \quad \gamma_{am,PP} = \frac{w_{am,PP}}{w_{PCP} + w_{am,PP}}$$

The amorphous densities of the extracted samples were obtained according to:

$$d_{am} = \frac{w_{am,PP}}{V_{s,x} - (w_{cr} V_{s,cr})}$$

The value of d_{am} and V_s for iPP and its blends with PCP before and after extraction are reported in Table 2. The density variation of iPP and iPP/PCP blends, after extraction, as a function of starting PCP content in the blends (measured before extraction) is shown in Figure 2. It can be seen that the density of iPP/PCP blends decreases with increase of PCP.

Wide-angle X-ray scattering studies

WAXS scans, from $2\theta = 8$ to 31° , of the isothermally crystallized samples showed the typical profile of iPP crystallized in the α -form⁹. For the blends the intensity of the crystalline peaks was reduced, whereas the hatched area, which includes the contribution of the continuous scattering of the amorphous iPP and PCP fractions, increased (Figure 3). The apparent crystal size D of iPP in

Table 2 Density of amorphous fraction (d_{am}) and total specific volume (V_s) of plain iPP and blends, before and after extraction

iPP/PCP	d_{am} (g cm ⁻³)	V_s (cm ³ g ⁻¹)
Before extraction		
100/0	0.85	1.11
90/10	0.88	1.09
70/30	0.95	1.06
50/50	1.00	1.02
Extracted		
100/0	0.72	1.20
90/10	0.61	1.34
70/30	0.49	1.55
50/50	0.30	2.15

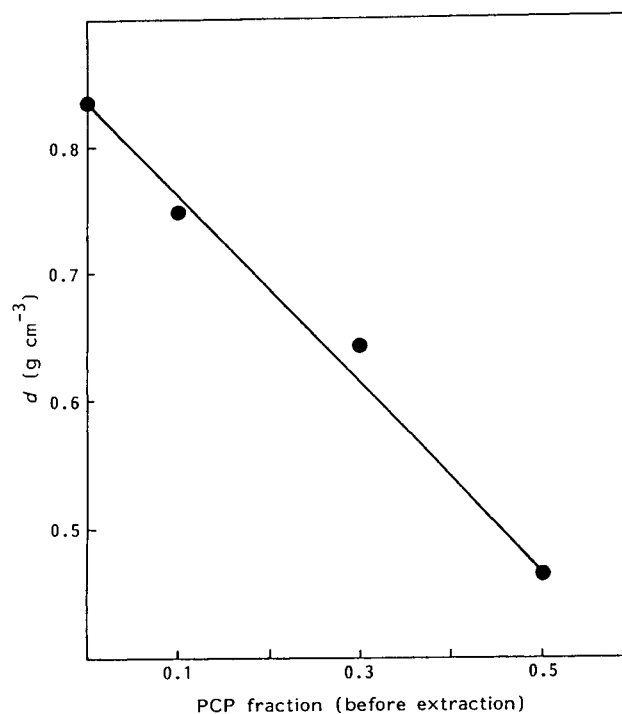


Figure 2 Density of iPP and iPP/PCP blends, after chloroform extraction, versus the original PCP weight fraction

the direction perpendicular to the (1 10), (1 30) and (0 40) crystallographic planes was calculated by the Scherrer equation¹⁰:

$$D = \frac{K\lambda}{\beta_0 \cos \theta}$$

where β_0 is the halfwidth in radians of the reflection corrected for instrumental broadening; λ is the wavelength of the X-radiation employed (1.542 Å); and K is a constant approximately equal to unity.

The crystal size D of non-extracted samples did not seem to be influenced by the PCP content, whereas the solvent-extracted samples showed lower crystal size values for the (1 30) and (1 10) crystal planes (Table 3). The presence of (2 20) reflection allowed the correction for lattice distortion of $D_{\langle 110 \rangle}$. As proposed by Morosoff *et al.*¹¹, we alternatively considered the possible contribution of paracrystallinity and microstrain. The microstrain contribution increased linearly with the order of reflection (n) and the paracrystalline contribution with the square of the order. The microstrain and paracrystalline factors (M_F , P_F) were obtained from:

$$M_F = \frac{1}{(\delta S_0^2)^{1/2} D_{\langle 110 \rangle}} \quad P_F = \frac{1}{\delta S_0 D_{\langle 110 \rangle}}$$

where δS_0^2 and δS_0 are respectively the intercepts of the ΔS^2 and ΔS versus n^2 plots (Figure 4), and ΔS was obtained by:

$$\Delta S = (\cos \theta) \beta_0 / \lambda$$

The paracrystallinity correction of the extracted and non-extracted samples was quite low, whereas the microstrain correction of the extracted blends appeared

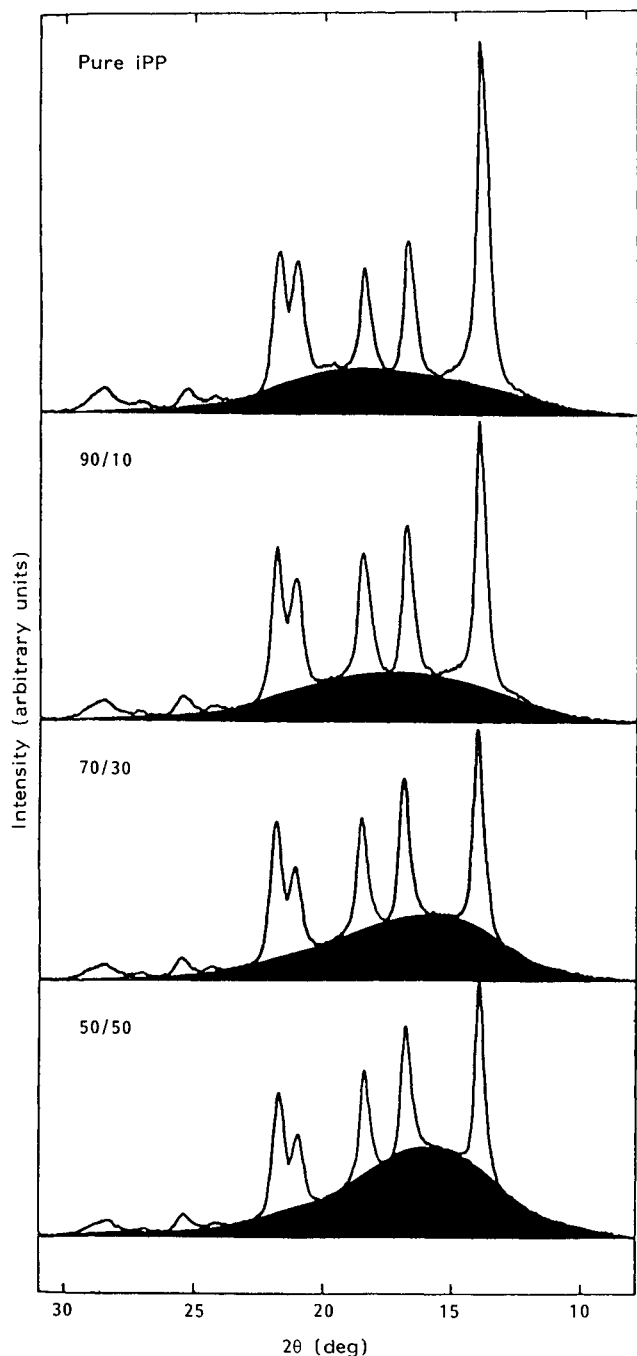


Figure 3 Wide-angle X-ray diffraction of pure iPP and iPP/PCP blends

Table 3 Apparent crystal size (*D*) of plain iPP and blends before and after extraction

iPP/PCP	<i>D</i> (Å)		
	(110)	(130)	(040)
Before extraction			
100/0	214	227	227
90/10	229	229	234
70/30	211	226	222
50/50	237	239	225
Extracted			
100/0	175	196	221
90/10	171	171	211
70/30	191	187	210
50/50	195	189	212

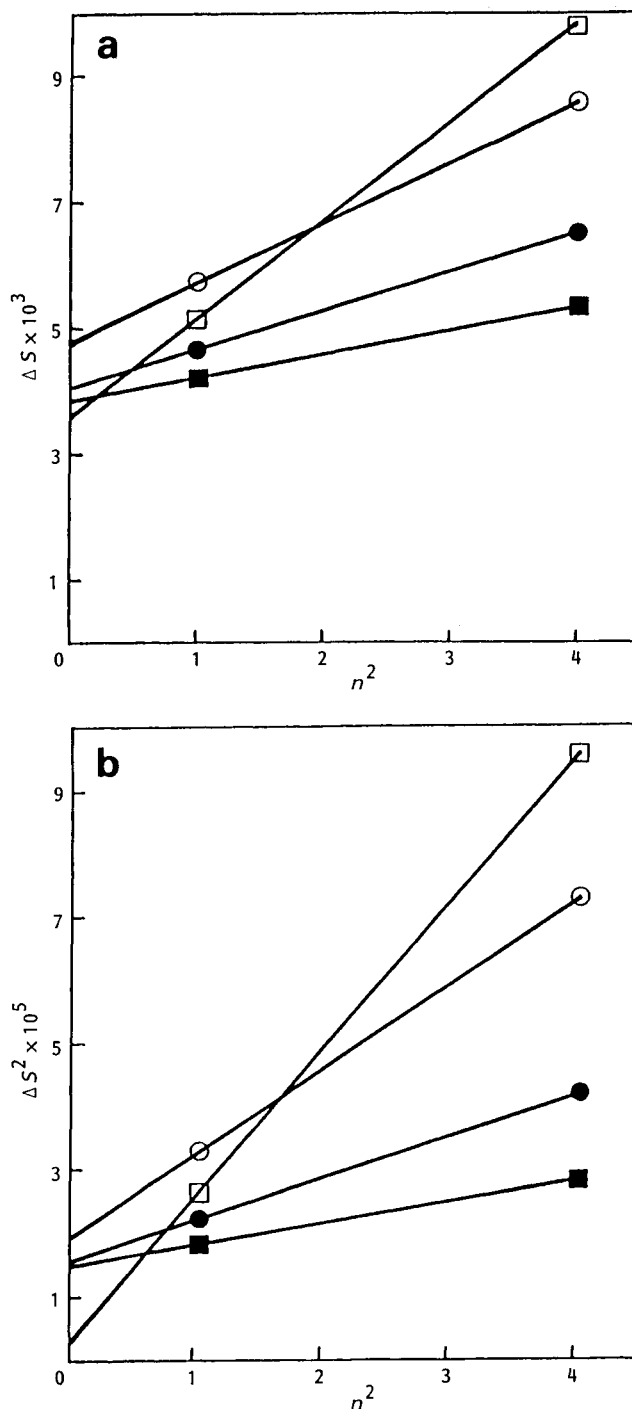


Figure 4 (a) Paracrystallinity and (b) microstrain plots: pure iPP before (●) and after (○) extraction; iPP/PCP 50/50 before (■) and after (□) extraction

to be much more significant (Table 4). This microstrain increase showed the disturbing action of the solvent on the iPP phase and accounts for the lower value of *D* observed in the case of iPP and iPP/PCP samples after extraction (see Table 3) and then for the trend of *T_m* shown by Figure 1.

Small-angle X-ray scattering studies

For all SAXS measurements the abscissa unit used was *Q*:

$$Q = 4\pi(\sin \theta)/\lambda$$

Table 4 Paracrystalline and microstrain factors (P_F and M_F) of plain iPP and blends before and after extraction

iPP/PCP	P_F	M_F
Before extraction		
100/0	1.15	1.20
90/10	1.16	1.32
70/30	1.13	1.17
50/50	1.10	1.11
Extracted		
100/0	1.20	1.30
90/10	1.37	2.08
70/30	1.43	2.92
50/50	1.44	2.95

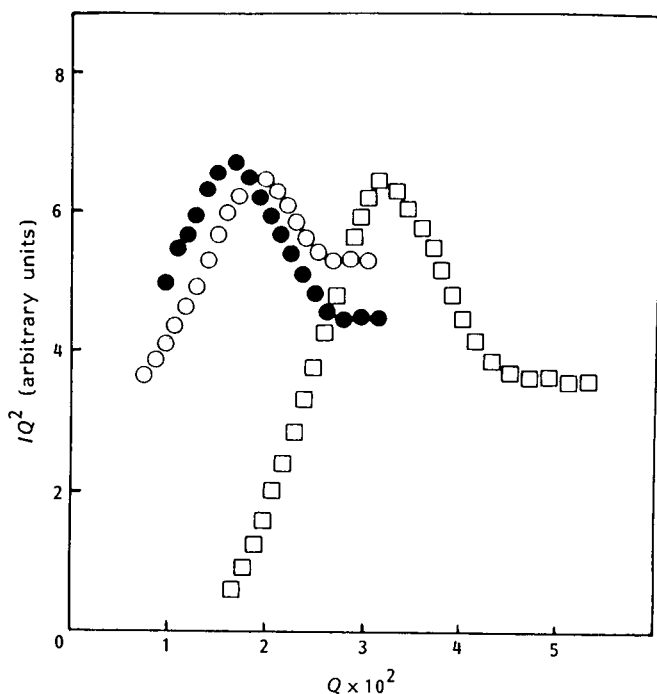


Figure 5 Plots of Lorentz-corrected desmeared intensity (IQ^2 versus Q) for non-extracted iPP/PCP blends: (\square) 90/10; (\circ) 70/30; (\bullet) 50/50

After Lorentz correction of the desmeared intensities¹², the long period L was calculated by:

$$L = 2\pi/Q_m$$

where Q_m is the abscissa value at the maximum of the plot.

The long period, defined as the distance between the centres of two adjacent lamellae, increased as a function of PCP content in the blends (see Figure 5 and Table 5). It is interesting to point out that all extracted blends showed the same long period value. Such a value turns out to be higher than that of extracted plain iPP (310 and 230 Å respectively).

The radius of gyration (R) can be assumed as a measure of the spatial extent of a whole particle. It is obtained from the innermost part of the scattering curve using the approximation of Guinier and Fournet¹³:

$$I(Q) = I_0 \exp(-Q^2 R^2/3)$$

where I_0 and $I(Q)$ are the intensities at angle zero and angle Q , respectively. From the slope (α) of the

Guinier plot $\ln I(Q)$ vs. Q^2 (Figure 6), the radius of gyration can be obtained as:

$$R = (-3 \tan \alpha)^{1/2}$$

Considering the elongated shape of particles, the radius of gyration of the cross section (R_c) can be calculated by applying the approximation of Guinier and Fournet^{14,15}:

$$I(Q) = [I(Q)Q]_0 \exp(-Q^2 R_c^2/2)$$

where $[I(Q)Q]_0$ is the product $I(Q)Q$ at zero angle. From the slope (α) of the $\ln I(Q)Q$ vs. Q^2 plot (Figure 7), the radius of gyration of the cross section is calculated as:

$$R_c = (-2 \tan \alpha)^{1/2}$$

Likewise, for lamellar particles¹⁴, from the Guinier approximation, the radius of gyration of the thickness (R_t) can be calculated by applying:

$$I(Q) = [I(Q)Q^2]_0 \exp(-Q^2 R_t^2)$$

where $[I(Q)Q^2]_0$ is the product $I(Q)Q^2$ at zero angle.

Table 5 Long period, particle and lamellar values of plain iPP and blends, before and after extraction (values in angstrom)

iPP/PCP	L	R	R_c	R_t	t	l_R	b_R
Before extraction							
100/0	200	94	49	31	107	277	131
90/10	195	95	50	26	90	280	148
70/30	310	89	44	27	94	268	120
50/50	370	93	50	25	87	272	150
Extracted							
100/0	230	90	44	29	100	272	115
90/10	310	92	49	25	87	270	146
70/30	310	88	50	28	97	251	143
50/50	310	89	54	27	94	245	162

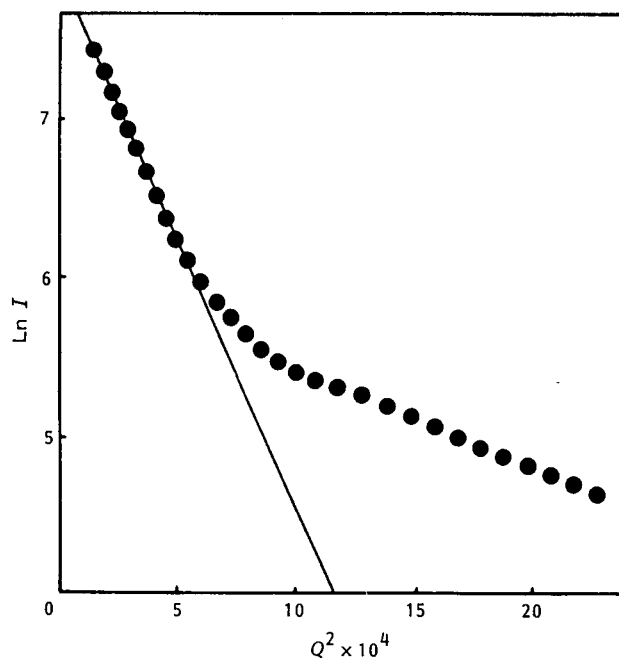


Figure 6 Plot of the radius of gyration (R) of iPP/PCP 50/50 non-extracted blend

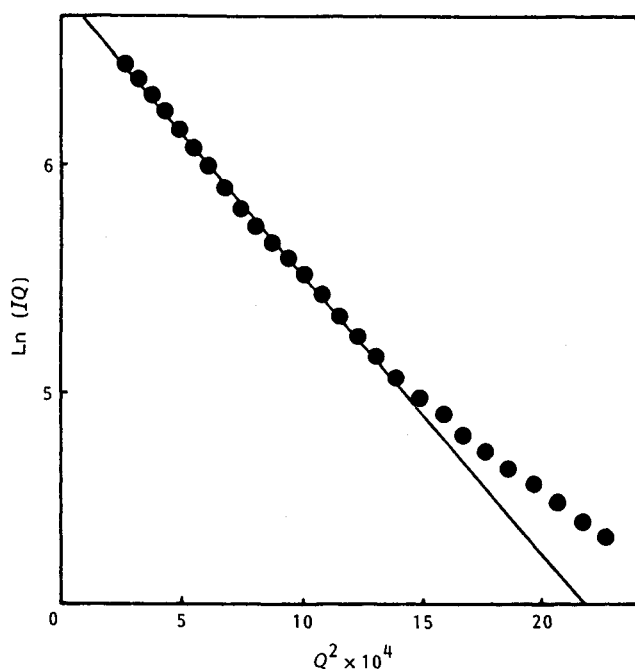


Figure 7 Plot of the radius of gyration of the cross section (R_c) of iPP/PCP 90/10 extracted blend

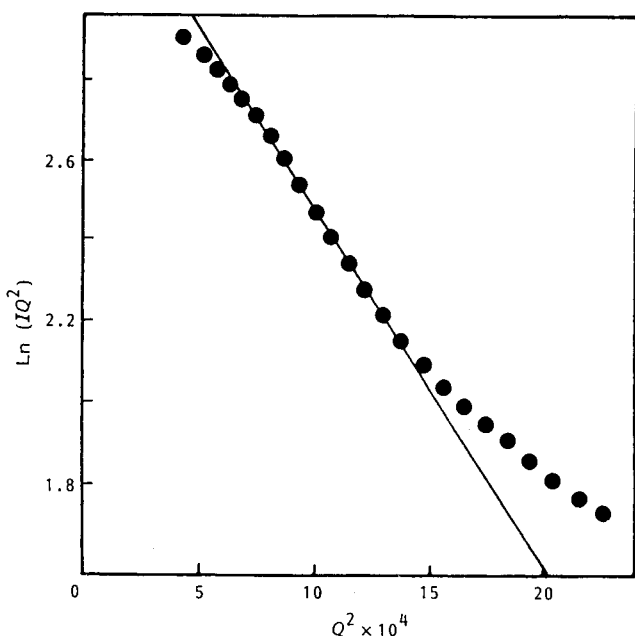


Figure 8 Plot of the radius of gyration of the thickness (R_t) of iPP/PCP 70/30 extracted blend

From the slope (α) of $\ln I(Q)Q^2$ vs. Q^2 plots (Figure 8), the R_t value can be obtained as:

$$R_t = (-1 \tan \alpha)^{1/2}$$

and the lamellar thickness t :

$$t = \sqrt{12} R_t$$

According to Kratky¹⁶, by the approximation of the particle to a parallelepiped, the lamellar length (l_R) and width (b_R) can be obtained from the three radii of gyration

(R , R_c , R_t) by:

$$l_R^2 = 12(R^2 - R_c^2)$$

$$b_R^2 = 12(R_c^2 - R_t^2)$$

The results are reported in Table 5.

As shown by the trends of the plots of Figure 9 the long period L as well as the thickness of amorphous interlamellar regions ($l_a = L - t$) of the blends increased as a function of PCP content. The lamellar thickness, in contrast, is independent of blend composition. Such a result strongly suggests that the uncrystallizable PCP component is located in interlamellar regions where with uncrystallized iPP it forms a homogeneous solid solution.

All extracted blends showed the same L values, which indicates that the solvent treatment, to remove the PCP component, rearranges the iPP structure. Owing to the chloroform-PCP affinity and to the good PCP distribution in the amorphous iPP, the solvent can realize a good diffusion and therefore interference in the blends. The pure iPP showed lower interference, since the solvent-carrier action of PCP is absent.

The values of R , R_c and R_t were quite similar for pure iPP and blends; extraction did not substantially modify the values. The values we obtained for the parameters of crystal dimensions normal to the thickness direction (l_R and b_R) are further confirmation of the hypothesis of a lamellar model.

CONCLUSIONS

The results reported in the present paper are in good agreement with the hypothesis of compatibility between amorphous iPP and PCP. The presence of PCP during crystallization and solvent treatment does not modify lamellar dimensions. The structure of all extracted blends is a repetition of lamellae with similar amorphous phases and is increasingly affected by microstrain with increasing PCP fraction.

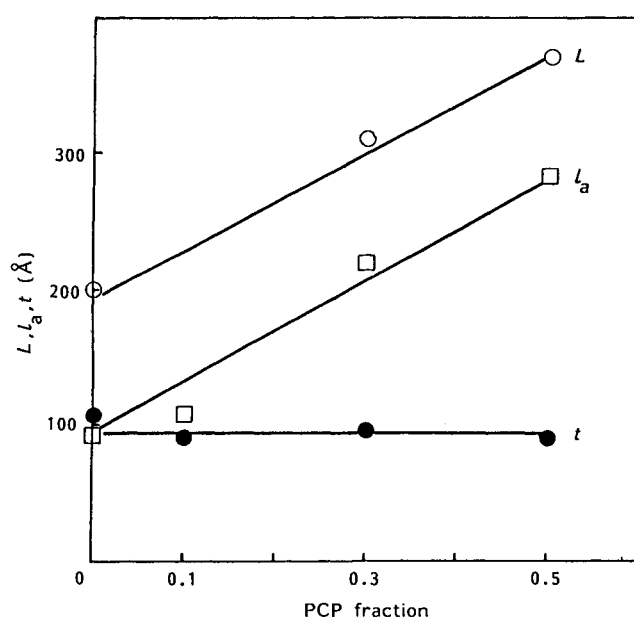


Figure 9 Long period L (○), amorphous thickness $l_a = L - t$ (□) and lamellar thickness t (●) versus PCP weight fraction (non-extracted blends)

A swollen polypropylene with a new structure and new characteristics can be obtained by chloroform extraction of iPP/PCP blends. The density and porosity of extracted iPP are connected with the original PCP content in the blends.

REFERENCES

- 1 Martuscelli, E., Silvestre, C., Canetti, M., de Lalla, C., Bonfatti, A. and Seves, A. *Makromol. Chem.* accepted
- 2 Seves, A., Vicini, L., Canetti, M. and Sadocco, P. *Colloid Polym. Sci.* 1980, **258**, 1126
- 3 Martuscelli, E., Canetti, M., Vicini, L. and Seves, A. *Polymer* 1982, **23**, 331
- 4 Galli, R., Canetti, M., Sadocco, P., Seves, A. and Vicini, L. *J. Polym. Sci., Polym. Phys. Edn.* 1983, **21**, 717
- 5 Danusso, F., Moraglio, G., Ghiglia, N., Motta, L. and Talamini, G. *Chim. Ind.* 1959, **8**, 7
- 6 Schnabel, E., Hosemann, R. and Rode, B. *J. Appl. Phys.* 1972, **43**, 3237
- 7 Glatter, O. *J. Appl. Crystallogr.* 1974, **17**, 147
- 8 Van Krevelen, D. W. 'Properties of Polymers', Elsevier, Amsterdam, 1976
- 9 Turner Jones, A., Aizlewood, J. M. and Beckett, D. R. *Makromol. Chem.* 1964, **75**, 134
- 10 Alexander, L. E. 'X-ray Diffraction Methods in Polymer Science', Wiley Interscience, New York, 1969
- 11 Morosoff, N., Sakaoku, K. and Peterlin, A. *J. Polym. Sci. (A-2)* 1972, **10**, 1221
- 12 Vonk, C. G. *J. Appl. Crystallogr.* 1973, **6**, 81
- 13 Guinier, A. and Fournet, G. 'Small Angle Scattering of X-rays', Wiley Interscience, New York, 1955
- 14 Kratky, O. and Porod, G. *Acta Phys. Austr.* 1948, **2**, 133
- 15 Porod, G. *Acta Phys. Austr.* 1948, **2**, 255
- 16 Kratky, O. and Miholic, G. *J. Polym. Sci. (C)* 1963, **2**, 449